Gates, States, and Circuits:

Notes on the circuit model of quantum computation

Tech. Note 014v2 http://threeplusone.com/gates

Gavin E. Crooks

2019-07-08

Contents

1 Single qubit gates

Pauli-I (identity):

$$\text{—} \qquad \begin{pmatrix} 1 & 0 \\ 0 & 1 \end{pmatrix}$$

Pauli-X gate (X-gate, NOT, bit flip)

$$\text{—}\boxed{\text{X}}\text{—} \qquad \begin{pmatrix} 0 & 1 \\ 1 & 0 \end{pmatrix}$$

Pauli-Y gate (Y-gate) :

$$\text{—}\boxed{\text{Y}}\text{—} \qquad \begin{pmatrix} 0 & -i \\ i & 0 \end{pmatrix}$$

Useful mnemonic: "Minus eye high"

Pauli-Z gate (Z-gate, phase flip)

$$\text{—}\boxed{\text{Z}}\text{—} \qquad \begin{pmatrix} 1 & 0 \\ 0 & -1 \end{pmatrix}$$

S (Phase, P, 'ess') gate

$$\text{—}\boxed{\text{S}}\text{—} \qquad \begin{pmatrix} 1 & 0 \\ 0 & i \end{pmatrix}$$

T ("tee", $\pi/8$) gate

$$\text{—}\boxed{\text{T}}\text{—} \qquad \begin{pmatrix} 1 & 0 \\ 0 & e^{i\pi/4} \end{pmatrix}$$

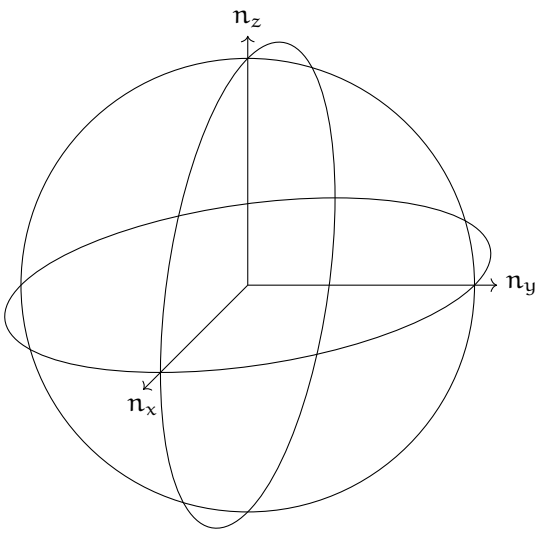

Figure 1: Sphere of 1-qubit gates. Each point within this sphere represents a unique (up to phase) 1-qubit gate. Antipodal points on the surface represent the same gate.

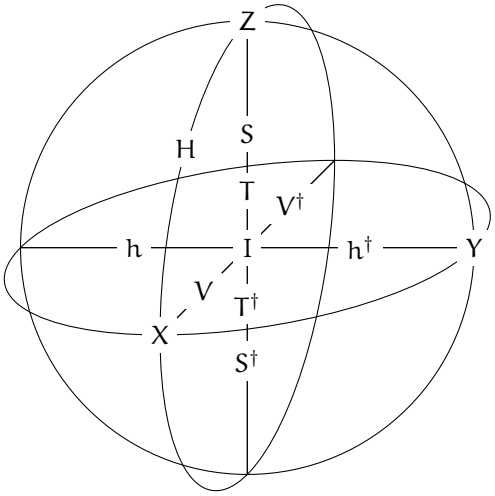

Figure 2: Coordinates of common 1-qubit gates

Hadamard gate

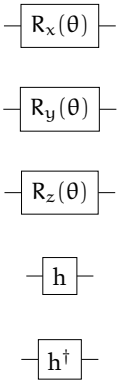

2 The canonical gate

The canonical gate is a 3-parameter quantum logic gate that acts on two qubits.

$$\begin{aligned}&\mathsf{CAN}(t_x, t_y, t_z)\\ &\quad = \exp\Big(-i\frac{\pi}{2}(t_x X\otimes X + t_y Y\otimes Y + t_z Z\otimes Z)\Big)\end{aligned} \quad (1)$$

Here, $X = \left(\begin{smallmatrix}0 & 1\\ 1 & 0\end{smallmatrix}\right)$, $Y = \left(\begin{smallmatrix}0 & -i\\ i & 0\end{smallmatrix}\right)$, and $Z = \left(\begin{smallmatrix}1 & 0\\ 0 & -1\end{smallmatrix}\right)$ are the 1-qubit Pauli matrices. Note that other choices for the prefactor in the exponential are also common in the literature.

The canonical gate is, in a sense, the elementary 2-qubit gate, since any other 2-qubit gate can be decomposed into a canonical gate, and local 1-qubit interactions [2, 3, 4, 5].

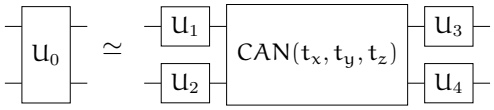

Here we use '$\simeq$' to indicate that two gates have the same unitary operator up to a global (and generally irrelevant) phase factor.

The canonical gate is periodic in each parameters with period 4, or period 2 if we neglect a -1 global phase factor. Thus we can constrain each parameter to the range $[-1, 1)$. Since $X\otimes X$, $Y\otimes Y$, and $Z\otimes Z$ all commute, the parameter space has the topology of a 3-torus.

However, the canonical coordinates of any given 2-qubit gate are not unique since we have considerable freedom in the prepended and postpended local gates. To remove these symmetries we can constraint the canonical parameters to a "Weyl chamber" [1, 1].

$$(\tfrac{1}{2} \geqslant t_x \geqslant t_y \geqslant t_z \geqslant 0) \cup (\tfrac{1}{2} \geqslant (1-t_x) \geqslant t_y \geqslant t_z > 0) \quad (2)$$

This Weyl chamber forms a trirectangular tetrahedron. All gates in the Weyl chamber are locally inequivalent (They cannot be obtained from each other via local 1-qubit gates). The net of the Weyl chamber is illustrated in Fig. 3, and the coordinates of many common 2-qubit gates are listed in table 1. Code for performing a canonical-decomposition, and therefore of determining the Weyl coordinates, can be found in the decompositions subpackage of `QuantumFlow` [6].

3 Principal 2-qubit gates

We use '$\cong$' to indicate that two gates are locally equivalent, in that they can be mapped to one another by local,

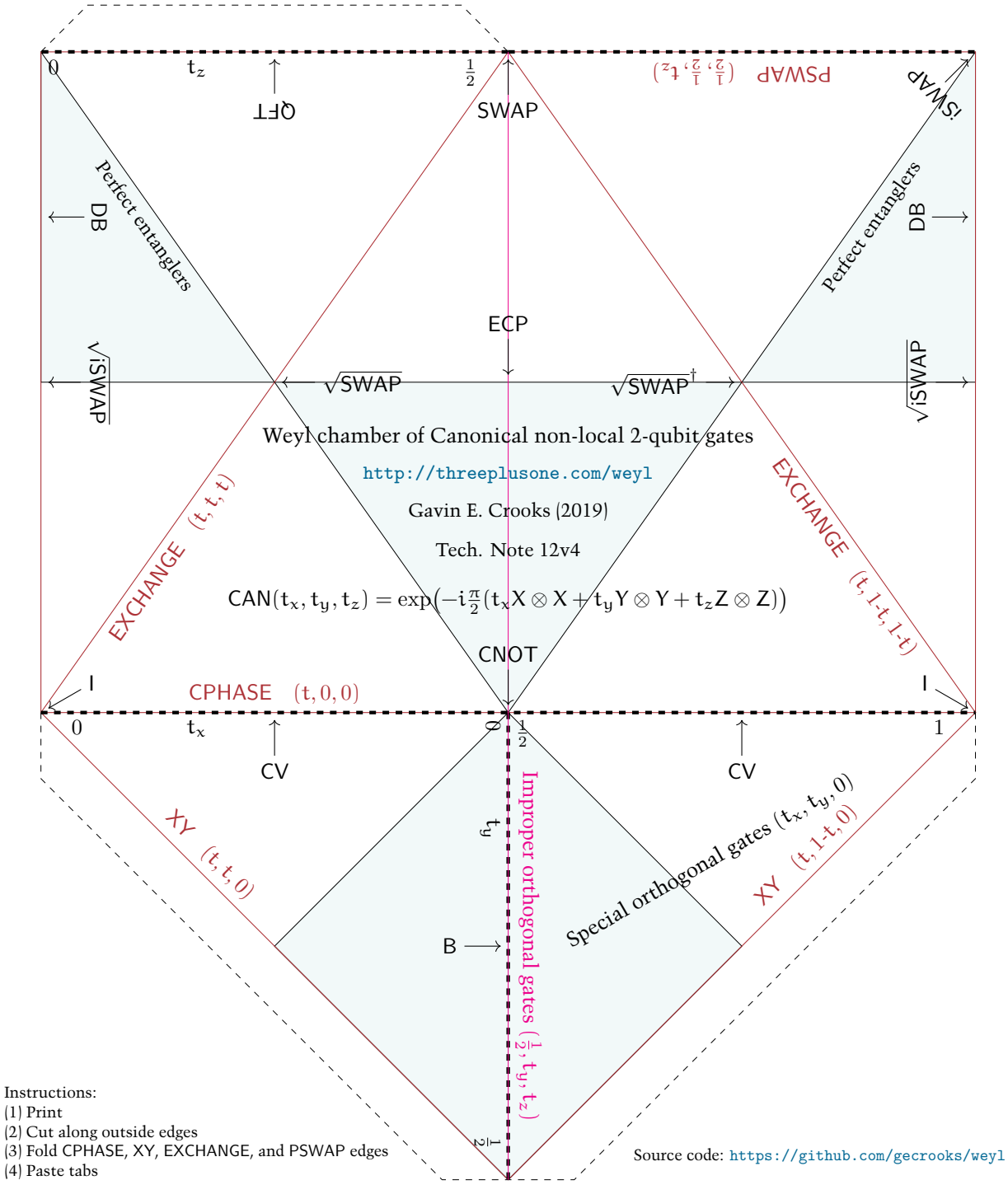

Figure 3: The Weyl chamber of canonical non-local 2 qubit gates. (Print, cut, fold, and paste)

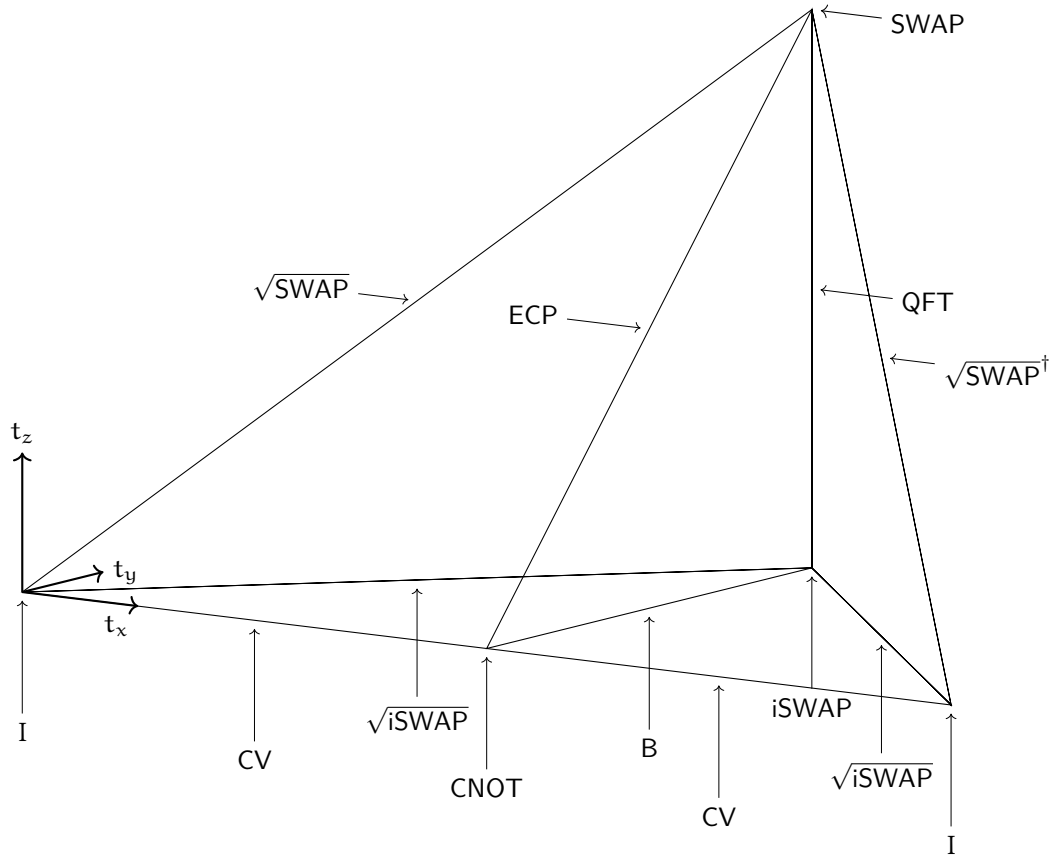

Figure 4: Location of the 11 principal 2-qubit gates in the Weyl chamber. All of these gates have coordinates of the form $\mathrm{CAN}(\frac{1}{4}\mathrm{k_x}, \frac{1}{4}\mathrm{k_y}, \frac{1}{4}\mathrm{k_z})$, for integer $\mathrm{k_x}$, $\mathrm{k_y}$, and $\mathrm{k_z}$. Note there is a symmetry on the bottom face such that $\mathrm{CAN}(\mathrm{t_x}, \mathrm{t_y}, 0) \cong \mathrm{CAN}(\frac{1}{2} - \mathrm{t_x}, \mathrm{t_y}, 0)$.

Table 1: Canonical coordinates of common 2-qubit gates

Gate	t_x $\leqslant\frac{1}{2}$	t_y	t_z	t'_x $>\frac{1}{2}$	t'_y	t'_z
I_2	0	0	0	1	0	0
CNOT / CZ / MS	$\frac{1}{2}$	0	0			
iSWAP / DCNOT	$\frac{1}{2}$	$\frac{1}{2}$	0	$\frac{3}{4}$	$\frac{1}{2}$	0
SWAP	$\frac{1}{2}$	$\frac{1}{2}$	$\frac{1}{2}$			
CV	$\frac{1}{4}$	0	0	$\frac{3}{4}$	0	0
$\sqrt{\text{iSWAP}}$	$\frac{1}{4}$	$\frac{1}{4}$	0	$\frac{3}{4}$	$\frac{1}{4}$	0
DB	$\frac{3}{8}$	$\frac{3}{8}$	0	$\frac{5}{8}$	$\frac{3}{8}$	0
$\sqrt{\text{SWAP}}$	$\frac{1}{4}$	$\frac{1}{4}$	$\frac{1}{4}$			
$\sqrt{\text{SWAP}}^\dagger$				$\frac{3}{4}$	$\frac{1}{4}$	$\frac{1}{4}$
B	$\frac{1}{2}$	$\frac{1}{4}$	0			
ECP	$\frac{1}{2}$	$\frac{1}{4}$	$\frac{1}{4}$			
QFT_2	$\frac{1}{2}$	$\frac{1}{2}$	$\frac{1}{4}$			
Ising / CPHASE	t	0	0			
XY	t	t	0	t	1-t	0
Exchange / SWAP^α	t	t	t	t	1-t	1-t
PSWAP	$\frac{1}{2}$	$\frac{1}{2}$	t			
Special orthogonal	t_x	t_y	0			
Improper orthogonal	$\frac{1}{2}$	t_y	t_z			
XXY	t	t	δ	t	1-t	δ
	δ	t	t	δ	t	t

1-qubit rotations.

3.1 Clifford gates

There are four unique 2-qubits gates in the Clifford group (up to local 1-qubit Cliffords): the identity, CNOT, iSWAP, and SWAP gates.

Identity gate

$$I_2 = \begin{pmatrix} 1&0&0&0\\ 0&1&0&0\\ 0&0&1&0\\ 0&0&0&1 \end{pmatrix} = \text{CAN}(0,0,0) \tag{3}$$

Controlled-NOT gate (CNOT, controlled-X, CX)

$$\text{CNOT} = \begin{pmatrix} 1&0&0&0\\ 0&1&0&0\\ 0&0&0&1\\ 0&0&1&0 \end{pmatrix} \cong \text{CAN}(\tfrac{1}{2},0,0) \tag{4}$$

Commonly represented by the circuit diagrams

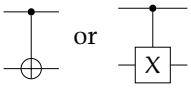

The CNOT gate is not symmetric between the two qubits. But we can switch control • and target ⊕ with local Hadamard gates.

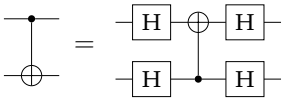

iSWAP-gate

$$\text{iSWAP} = \begin{pmatrix} 1&0&0&0\\ 0&0&i&0\\ 0&i&0&0\\ 0&0&0&1 \end{pmatrix} \simeq \text{CAN}(\tfrac{1}{2},\tfrac{1}{2},0) \tag{5}$$

SWAP-gate

$$\text{SWAP} = \begin{pmatrix} 1&0&0&0\\ 0&0&1&0\\ 0&1&0&0\\ 0&0&0&1 \end{pmatrix} \simeq \text{CAN}(\tfrac{1}{2},\tfrac{1}{2},\tfrac{1}{2}) \tag{6}$$

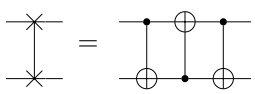

3.2 XX gates

Gates in the XX (or Ising) class have coordinates $\text{CAN}(t,0,0)$, which forms the front edge of the Weyl chamber. This includes the identity and CNOT gates.

XX gate (Ising)

$$\begin{aligned}\mathrm{XX}(t) &= e^{-i\frac{\pi}{2}t\,X\otimes X} \\ &= \begin{pmatrix} \cos(\frac{\pi}{2}t) & 0 & 0 & -i\sin(\frac{\pi}{2}t) \\ 0 & \cos(\frac{\pi}{2}t) & -i\sin(\frac{\pi}{2}t) & 0 \\ 0 & -i\sin(\frac{\pi}{2}t) & \cos(\frac{\pi}{2}t) & 0 \\ -i\sin(\frac{\pi}{2}t) & 0 & 0 & \cos(\frac{\pi}{2}t) \end{pmatrix} \\ &= \mathrm{CAN}(t,0,0)\end{aligned} \tag{7}$$

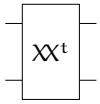

Mølmer-Sørensen gate (MS) [? ?]

$$\begin{aligned}\mathrm{MS} &= \frac{1}{\sqrt{2}}\begin{pmatrix} 1 & 0 & 0 & i \\ 0 & 1 & i & 0 \\ 0 & i & 1 & 0 \\ i & 0 & 0 & 1 \end{pmatrix} \\ &= \mathrm{CAN}(-\tfrac{1}{2},0,0) \\ &\cong \mathrm{CAN}(\tfrac{1}{2},0,0) \\ &\cong \mathrm{CNOT}\end{aligned} \tag{8}$$

Proposed as a natural gate for laser driven trapped ions. Locally equivalent to CNOT. The Mølmer-Sørensen gate, or more exactly its complex conjugate $\mathrm{MS}^\dagger = \mathrm{CAN}(\frac{1}{2},0,0)$ is the natural canonical representation of the CNOT/CZ/MS gate family.

Magic gate (M) [1, 1, 1]

$$\mathrm{M} = \frac{1}{\sqrt{2}}\begin{pmatrix} 1 & i & 0 & 0 \\ 0 & 0 & i & 1 \\ 0 & 0 & i & -1 \\ 1 & -i & 0 & 0 \end{pmatrix} \tag{9}$$

$$\cong \mathrm{CAN}(\tfrac{1}{2},0,0) \tag{10}$$

[7]

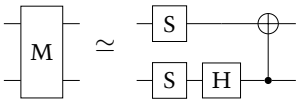

YY gate

$$\begin{aligned}\mathrm{YY}(t) &= e^{-i\frac{\pi}{2}t\,Y\otimes Y} \\ &= \begin{pmatrix} \cos(\frac{\pi}{2}t) & 0 & 0 & +i\sin(\frac{\pi}{2}t) \\ 0 & \cos(\frac{\pi}{2}t) & -i\sin(\frac{\pi}{2}t) & 0 \\ 0 & -i\sin(\frac{\pi}{2}t) & \cos(\frac{\pi}{2}t) & 0 \\ +i\sin(\frac{\pi}{2}t) & 0 & 0 & \cos(\frac{\pi}{2}t) \end{pmatrix} \\ &= \mathrm{CAN}(0,t,0) \\ &\cong \mathrm{CAN}(t,0,0)\end{aligned} \tag{11}$$

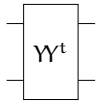

ZZ gate

$$\begin{aligned}\mathrm{ZZ}(t) &= e^{-i\frac{\pi}{2}t\,Z\otimes Z} \\ &= \begin{pmatrix} 1 & 0 & 0 & 0 \\ 0 & e^{-i\pi t} & 0 & 0 \\ 0 & 0 & e^{-i\pi t} & 0 \\ 0 & 0 & 0 & 1 \end{pmatrix} \\ &= \mathrm{CAN}(0,0,t) \\ &\cong \mathrm{CAN}(t,0,0)\end{aligned} \tag{12}$$

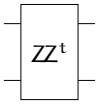

Controlled-Y gate

$$\begin{aligned}\mathrm{CY} &= \begin{pmatrix} 1 & 0 & 0 & 0 \\ 0 & 1 & 0 & 0 \\ 0 & 0 & 0 & -i \\ 0 & 0 & +i & 0 \end{pmatrix} \\ &\cong \mathrm{CAN}(\tfrac{1}{2},0,0)\end{aligned} \tag{13}$$

Commonly represented by the circuit diagram:

Controlled-Z gate (CZ or CSIGN)

$$\begin{aligned}\mathrm{CZ} &= \begin{pmatrix} 1 & 0 & 0 & 0 \\ 0 & 1 & 0 & 0 \\ 0 & 0 & 1 & 0 \\ 0 & 0 & 0 & -1 \end{pmatrix} \\ &\cong \mathrm{CAN}(\tfrac{1}{2},0,0)\end{aligned} \tag{14}$$

Commonly represented by the circuit diagrams

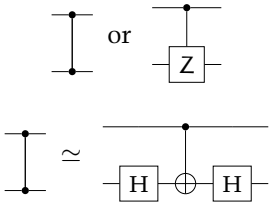

Controlled-V gate (square root of CNOT gate):

$$\begin{aligned}\mathrm{CV} &= \begin{pmatrix} 1 & 0 & 0 & 0 \\ 0 & 1 & 0 & 0 \\ 0 & 0 & \frac{1+i}{2} & \frac{1-i}{2} \\ 0 & 0 & \frac{1-i}{2} & \frac{1+i}{2} \end{pmatrix} \\ &\cong \mathrm{CAN}(\tfrac{1}{4},0,0)\end{aligned} \tag{15}$$

The CV gate is a square-root of CNOT, since the V-gate

is the square root of the X-gate

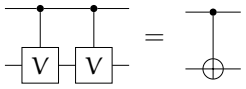

Note that the inverse $CV^\dagger$ is a distinct square-root of CNOT. However CV and $CV^\dagger$ are locally equivalent, which is a consequence of the symmetry about $t_x = \frac{1}{2}$ on the bottom face of the Weyl chamber.

3.3 XY gates

Gates in the XY class forms two edges of the Weyl chamber with coordinates $\mathrm{CAN}(t, t, 0)$ (for $t \leqslant \frac{1}{2}$) and $\mathrm{CAN}(t, 1-t, 0)$ (for $t > \frac{1}{2}$). This includes the identity and iSWAP gates.

XY-gate Also occasionally referred to as the piSWAP (or parametric iSWAP) gate.

$$\begin{aligned}\mathrm{XY}(t) &= \begin{pmatrix} 1 & 0 & 0 & 0 \\ 0 & \cos(\pi t) & -i\sin(\pi t) & 0 \\ 0 & -\sin(\pi t) & \cos(\pi t) & 0 \\ 0 & 0 & 0 & 1 \end{pmatrix} \\ &= \mathrm{CAN}(t, t, 0) \\ &\cong \mathrm{CAN}(t, 1-t, 0)\end{aligned} \tag{16}$$

Double Controlled NOT gate (DCNOT)

$$\begin{aligned}\mathrm{DCNOT} &= \begin{pmatrix} 1 & 0 & 0 & 0 \\ 0 & 0 & 0 & 1 \\ 0 & 1 & 0 & 0 \\ 0 & 0 & 1 & 0 \end{pmatrix} \\ &\cong \mathrm{CAN}(\tfrac{1}{2}, \tfrac{1}{2}, 0)\end{aligned} \tag{17}$$

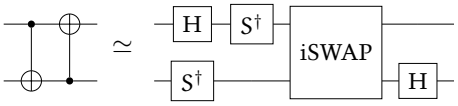

bSWAP (Bell-Rabi) gate [?]

$$\begin{aligned}\mathrm{bSWAP} &= \begin{pmatrix} 0 & 0 & 0 & -i \\ 0 & 1 & 0 & 0 \\ 0 & 0 & 1 & 0 \\ -i & 0 & 0 & 0 \end{pmatrix} \\ &= \mathrm{CAN}(\tfrac{1}{2}, -\tfrac{1}{2}, 0) \\ &\cong \mathrm{CAN}(\tfrac{1}{2}, \tfrac{1}{2}, 0)\end{aligned} \tag{18}$$

Dagwood Bumstead (DB) gate [8] Of all the gates in the XY class, the Dagwood Bumstead-gate makes the biggest sandwiches. [8, Fig. 4]

$$\begin{aligned}\mathrm{DB} &= \begin{pmatrix} 1 & 0 & 0 & 0 \\ 0 & \cos(\frac{3\pi}{8}) & -i\sin(\frac{3\pi}{8}) & 0 \\ 0 & -\sin(\frac{3\pi}{8}) & \cos(\frac{3\pi}{8}) & 0 \\ 0 & 0 & 0 & 1 \end{pmatrix} \\ &= \mathrm{XY}(\tfrac{3}{8}) \\ &= \mathrm{CAN}(\tfrac{3}{8}, \tfrac{3}{8}, 0)\end{aligned} \tag{19}$$

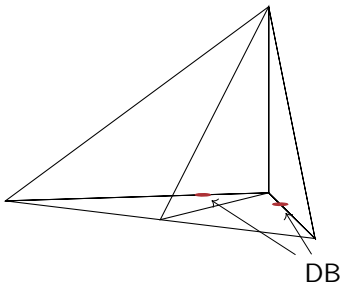

3.4 Exchange-interaction gates

Includes the identity and SWAP gates.

EXCH (XXX) gate

$$\mathrm{EXCH}(t) = \mathrm{CAN}(t, t, t) \tag{20}$$

SWAP-alpha gates

$$\mathrm{SWAP}^\alpha \cong \mathrm{CAN}(\alpha, \alpha, \alpha) \tag{21}$$

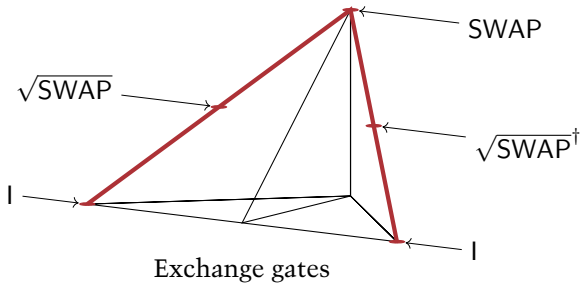

Exchange gates

√SWAP-gate

$$\begin{aligned}\sqrt{\mathrm{SWAP}} &= \begin{pmatrix} 1 & 0 & 0 & 0 \\ 0 & \frac{1}{2}(1+i) & \frac{1}{2}(1-i) & 0 \\ 0 & \frac{1}{2}(1-i) & \frac{1}{2}(1+i) & 0 \\ 0 & 0 & 0 & 1 \end{pmatrix} \\ &= \mathrm{CAN}(\tfrac{1}{4}, \tfrac{1}{4}, \tfrac{1}{4})\end{aligned} \tag{22}$$

Inverse √SWAP-gate

$$\begin{aligned}\sqrt{\mathrm{SWAP}}^\dagger &= \begin{pmatrix} 1 & 0 & 0 & 0 \\ 0 & \frac{1}{2}(1-i) & \frac{1}{2}(1+i) & 0 \\ 0 & \frac{1}{2}(1+i) & \frac{1}{2}(1-i) & 0 \\ 0 & 0 & 0 & 1 \end{pmatrix} \\ &= \mathrm{CAN}(\tfrac{3}{4}, \tfrac{1}{4}, \tfrac{1}{4})\end{aligned} \tag{23}$$

Because of the symmetry around $t_x = \frac{1}{2}$ on the base of the Weyl chamber, the CNOT and iSWAP gates only have one square root. But the SWAP has two unique square roots, which are inverses of each other.

3.5 Parametric SWAP gates

The class of parametric SWAP (PSWAP) gates forms the remaining edge of the Weyl chamber, connecting the SWAP

and iSWAP gates.

pSWAP gate [9]

$$\mathrm{pSWAP}(\theta) = \begin{pmatrix} 1 & 0 & 0 & 0 \\ 0 & 0 & e^{i\theta} & 0 \\ 0 & e^{i\theta} & 0 & 0 \\ 0 & 0 & 0 & 1 \end{pmatrix} \cong \mathrm{CAN}(\tfrac{1}{2}, \tfrac{1}{2}, \tfrac{1}{2} - \tfrac{\theta}{\pi}) \quad (24)$$

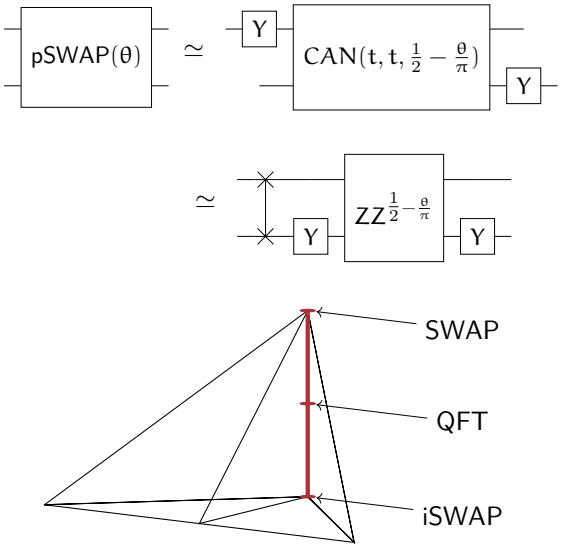

pSWAP gates

2-qubit quantum Fourier transform (QFT) [1]

$$\mathrm{QFT} = \frac{1}{2}\begin{pmatrix} 1 & 1 & 1 & 1 \\ 1 & i & -1 & -i \\ 1 & -1 & 1 & -1 \\ 1 & -i & -1 & i \end{pmatrix} \cong \mathrm{CAN}(\tfrac{1}{2}, \tfrac{1}{2}, \tfrac{1}{4}) \quad (25)$$

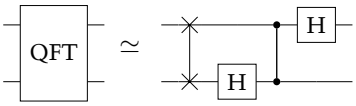

3.6 Orthogonal gates

An orthogonal gate, in this context, is a gate that can be represented by an orthogonal matrix (up to local 1-qubit rotations.) The special orthogonal gates have determinant $+1$ and coordinates $\mathrm{CAN}(t_x, t_y, 0)$, which covers the bottom surface of the canonical Weyl chamber.

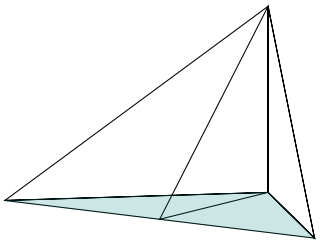

Special orthogonal gates

The improper orthogonal gates have determinant -1 and coordinates $\mathrm{CAN}(\frac{1}{2}, t_y, t_z)$, which is a plane connecting the CNOT, iSWAP, and SWAP gates.

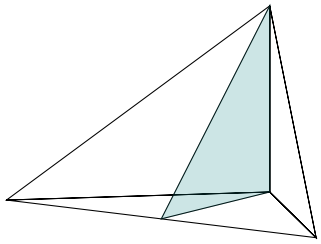

Improper orthogonal gates

B (Berkeley) gate [1]

$$B = \begin{pmatrix} \cos(\frac{\pi}{8}) & 0 & 0 & i\sin(\frac{\pi}{8}) \\ 0 & \cos(\frac{3\pi}{8}) & i\sin(\frac{3\pi}{8}) & 0 \\ 0 & i\sin(\frac{3\pi}{8}) & \cos(\frac{3\pi}{8}) & 0 \\ i\sin(\frac{\pi}{8}) & 0 & 0 & \cos(\frac{\pi}{8}) \end{pmatrix} \cong \mathrm{CAN}(\tfrac{1}{2}, \tfrac{1}{4}, 0) \quad (26)$$

Notably two-B gates are enough to create any other 2-qubit gate.

ECP-gate [8]

$$\mathrm{ECP} = \frac{1}{2}\begin{pmatrix} 2c & 0 & 0 & -i2s \\ 0 & (1+i)(c-s) & (1-i)(c+s) & 0 \\ 0 & (1-i)(c+s) & (1+i)(c-s) & 0 \\ -i2s & 0 & 0 & 2c \end{pmatrix} \quad (27)$$
$$c = \cos(\tfrac{\pi}{8}), \quad s = \sin(\tfrac{\pi}{8})$$
$$= \mathrm{CAN}(\tfrac{1}{2}, \tfrac{1}{4}, \tfrac{1}{4})$$

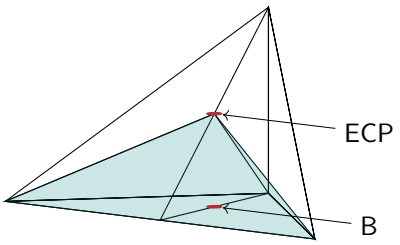

B and ECP gates, and ECP pyramid

3.7 XXY gates

The remaining faces of the Weyl chamber are the XXY family. Thanks to the Weyl symmetries, this family covers all three faces that meet at the SWAP gate.

$$\mathrm{XXY}(t, \delta) = \mathrm{CAN}(t, t, \delta) \quad (28)$$

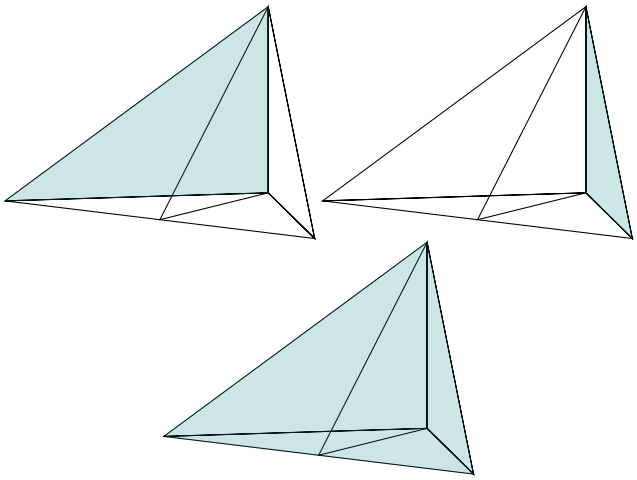

3.8 Perfect entanglers

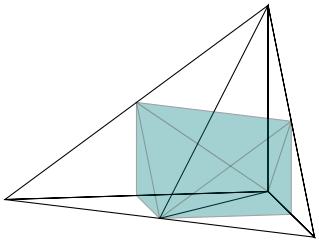

Perfect entaglers

4 Multi-qubit gates

Toffoli gate (controlled-controlled-not, CCNOT)

$$\begin{bmatrix} 1&0&0&0&0&0&0&0\\ 0&1&0&0&0&0&0&0\\ 0&0&1&0&0&0&0&0\\ 0&0&0&1&0&0&0&0\\ 0&0&0&0&1&0&0&0\\ 0&0&0&0&0&1&0&0\\ 0&0&0&0&0&0&0&1\\ 0&0&0&0&0&0&1&0 \end{bmatrix} \tag{29}$$

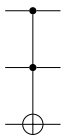

Fredkin gate (controlled-swap, CSWAP)

$$\begin{bmatrix} 1&0&0&0&0&0&0&0\\ 0&1&0&0&0&0&0&0\\ 0&0&1&0&0&0&0&0\\ 0&0&0&1&0&0&0&0\\ 0&0&0&0&1&0&0&0\\ 0&0&0&0&0&0&1&0\\ 0&0&0&0&0&1&0&0\\ 0&0&0&0&0&0&0&1 \end{bmatrix} \tag{30}$$

Table 2: Coordinates of the 24 1-qubit Clifford gates.

Gate	θ	n_x	n_y	n_z
I	0			
V	$\frac{1}{2}\pi$	1	0	0
X	π	1	0	0
$V^\dagger$	$-\frac{1}{2}\pi$	1	0	0
$h^\dagger$	$\frac{1}{2}\pi$	0	1	0
Y	π	0	1	0
h	$-\frac{1}{2}\pi$	0	1	0
S	$\frac{1}{2}\pi$	0	0	1
Z	π	0	0	1
$S^\dagger$	$-\frac{1}{2}\pi$	0	0	1
H	π	$\frac{1}{\sqrt{2}}$	$\frac{1}{\sqrt{2}}$	0
	π	$\frac{1}{\sqrt{2}}$	0	$\frac{1}{\sqrt{2}}$
	π	0	$\frac{1}{\sqrt{2}}$	$\frac{1}{\sqrt{2}}$
	π	$-\frac{1}{\sqrt{2}}$	$\frac{1}{\sqrt{2}}$	0
	π	$\frac{1}{\sqrt{2}}$	0	$-\frac{1}{\sqrt{2}}$
	π	0	$-\frac{1}{\sqrt{2}}$	$\frac{1}{\sqrt{2}}$
	$\frac{2}{3}\pi$	$\frac{1}{\sqrt{3}}$	$\frac{1}{\sqrt{3}}$	$\frac{1}{\sqrt{3}}$
	$-\frac{2}{3}\pi$	$\frac{1}{\sqrt{3}}$	$\frac{1}{\sqrt{3}}$	$\frac{1}{\sqrt{3}}$
	$\frac{2}{3}\pi$	$-\frac{1}{\sqrt{3}}$	$\frac{1}{\sqrt{3}}$	$\frac{1}{\sqrt{3}}$
	$-\frac{2}{3}\pi$	$-\frac{1}{\sqrt{3}}$	$\frac{1}{\sqrt{3}}$	$\frac{1}{\sqrt{3}}$
	$\frac{2}{3}\pi$	$\frac{1}{\sqrt{3}}$	$-\frac{1}{\sqrt{3}}$	$\frac{1}{\sqrt{3}}$
	$-\frac{2}{3}\pi$	$\frac{1}{\sqrt{3}}$	$-\frac{1}{\sqrt{3}}$	$\frac{1}{\sqrt{3}}$
	$\frac{2}{3}\pi$	$\frac{1}{\sqrt{3}}$	$\frac{1}{\sqrt{3}}$	$-\frac{1}{\sqrt{3}}$
	$-\frac{2}{3}\pi$	$\frac{1}{\sqrt{3}}$	$\frac{1}{\sqrt{3}}$	$-\frac{1}{\sqrt{3}}$

References

[1] [citation needed]. (pages 2, 2, 6, 6, 6, 8, and 8).

[2] Jun Zhang, Jiri Vala, Shankar Sastry, and K. Birgitta Whaley. Geometric theory of nonlocal two-qubit operations. *Phys. Rev. A*, 67:042313 (2003). doi:10.1103/PhysRevA.67.042313. arXiv:quant-ph/0209120. (page 2).

[3] Jun Zhang, Jiri Vala, Shankar Sastry, and K. Birgitta Whaley. Optimal quantum circuit synthesis from controlled-unitary gates. *Phys. Rev. A*, 69:042309 (2004). doi:10.1103/PhysRevA.69.042309. ArXiv:quant-ph/0308167. (page 2).

[4] M. Blaauboer and R. L. de Visser. An analytical decomposition protocol for optimal implementation of two-qubit entangling gates. *J. Phys. A : Math. Theor*, 41:395307 (2008). doi:10.1088/1751-8113/41/39/395307. arXiv:cond-mat/0609750. (page 2).

[5] Paul Watts, Maurice O'Connor, and Jiří Vala. Metric structure of the space of two-qubit gates, perfect entanglers and quantum control. *Entropy*, 15:1963–1984 (2013). doi:10.3390/e15061963. (page 2).

[6] Gavin E. Crooks. QuantumFlow: A Quantum Algorithms Development Toolkit (2019). `https://quantumflow.readthedocs.io/`. (page 2).

[7] Farrokh Vatan and Colin Williams. Optimal quantum circuits for general two-qubit gates. *Phys. Rev. A*, 69:032315 (2004). doi:10.1103/PhysRevA.69.032315. ArXiv:quant-ph/0308006. (page 6).

[8] Eric C. Peterson, Gavin E. Crooks, and Robert S. Smith. Fixed-depth two-qubit circuits and the monodromy polytope. arXiv:1904.10541. (pages 7, 7, and 8).

[9] Robert S. Smith, Michael J. Curtis, and William J. Zeng. A practical quantum instruction set architecture. ArXiv:1608.03355. (page 8).

`http://threeplusone.com/gates`

typeset on 2019-07-08 with XeTeX version 0.99999
fonts: Trump Mediaeval (text), Euler (math)
2 7 1 8 2 8 1 8 3